CHARRACTERISTICS OF THE BORA WIND UNDER DIFFERENT CONDITIONS OF THE LEE BACKGROUND FLOW

Mark Žagar[1,2] and Jože Rakovec[2]

[1] Meteorological Office, EARS, Ljubljana, Slovenia
[2] Department for meteorology, University in Ljubljana, Slovenia
E-mail: *mark.zagar@gov.si*

Abstract: There are several modifiers of the bora wind at the eastern coast of the Adriatic, but common to the majority of situations with bora are the cross-coast pressure gradient and cold advection on the continent. In this paper a detailed analysis of numerical model simulations of two cases with bora is presented in terms of the two aforementioned background state parameters, and additionally on the warm advection into the Adriatic basin. The results indicate that the speed of the bora wind offshore does not depend on the origin of the air within the jet. It is found that warm air from aloft can enter the accelerating streamline at the mountain ridge and continue as bora jet offshore. The pressure gradient across the mountain barrier is found to be an excellent indicator of the bora wind speed with correlation of up to 0.98.

Keywords: *bora, COAMPS*

1. INTRODUCTION

Advection of polar air masses towards the Balkan peninsula and the Adriatic manifests itself at the sea level as a cold and gusty easterly to northeasterly wind called bora. The time of onset and the general strength are conditioned by the synoptic situation. Local characteristics, like the surface shear and turbulence and the propagation speed of the bora front, are known to be influenced by the temperature of the underlying sea surface, or more precisely by the temperature difference between the air and the sea surface (e.g. Enger and Grisogono, 1998).

In this paper, we hypothesize that some of the bora properties may also be influenced by the state of the background flow in the lee. Particularly we are interested in finding signs of significant effects of the warm advection aloft to the bora jet below. For this purpose we chose two cases with strong bora wind which we analyze using high resolution numerical simulations. The criteria for selection of the two cases are obviously defined in a way to distinguish between the presence and absence of the warm advection into the northern Adriatic region.

2. ANALYSIS OF TWO CASES

Due to the nature of situations with bora, i.e. the cold air outbreak past the eastern flank of the Alps in the lower troposphere, we have initially hypothesized that occasionally the middle troposphere circulation might lag sufficiently for creating favorable conditions for coexistence of bora jet below the warm southeasterly or southerly lee background flow. The two cases, one when the bora jet penetrated the warm flow cushion and the other when the northeasterly flow was deep, are presented later in this section.

The primary tool for the mesoscale meteorological analysis of the two cases is COAMPS^{TM} atmospheric model (Hodur, 1997). The model run in two-nest configuration with 15 and 5km grid spacing was initialized and coupled with the ECMWF operational analyses at 6 hour frequency. The number of vertical levels is 48 with well resolved boundary layer, i.e. there are 13 levels in the lowest kilometer.

The first case of February 3-5, 2006 was characterized by a deep layer of NE flow. As seen in the satellite image (Fig. 1, left) and in the model (Fig. 2, left) the bad weather system retreats towards the SE and is replaced by clearing due to the northerly advection of dry air which is also expressed as a NE wind and bora at the surface.

In the second case of February 22-24, 2006, surface and lower troposphere flow turned towards NE while strong southerly shear aloft continued to cause advection of warm and humid air. This is evident in the satellite photo (Figs. 1 and 2, right) as mid-level cloud bands in SSW to NNE direction.

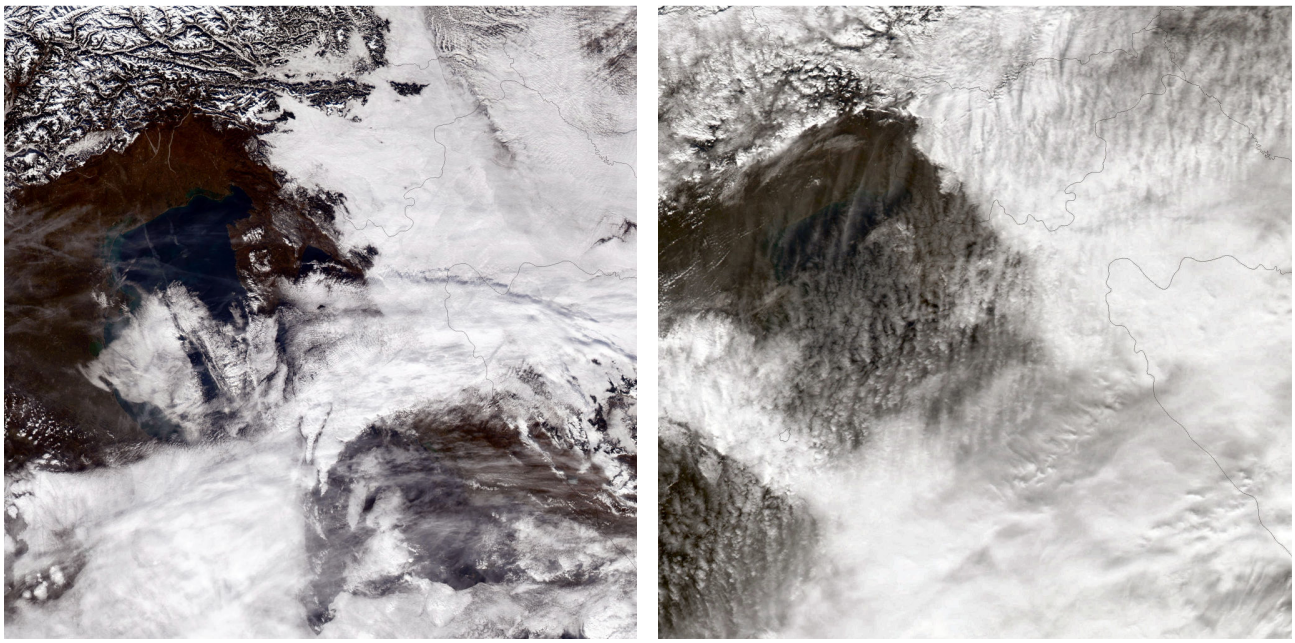

Figure 1: Satellite photo in visible spectrum (© NASA/MODIS) for 4 February 2006, 12UTC (left) and for 23 February 2006, 12:30UTC (right)

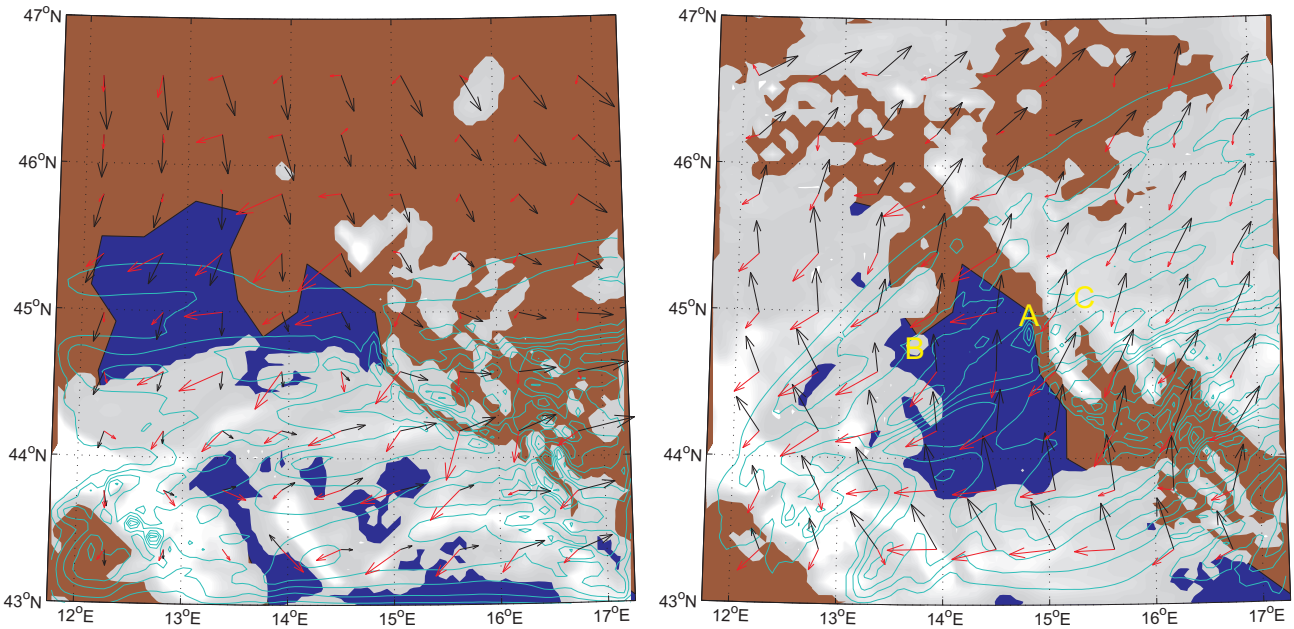

Figure 2: COAMPS simulated vertically integrated cloud water (gray shades) and cloud ice (cyan contours), both starting at 0.1g/kg; black arrows represent wind at around 4km above ground and red arrows represent wind at 10m above ground. The time of validity is the same as in Fig. 1.

Our main interest lies in evaluating the differences in bora wind speed along the streamline starting at the coast at point A in Fig. 2, especially during the early stages of the bora episodes when the lee background conditions are assumed to play a role.

Figure 3 illustrates the temperature advection into the atmospheric column above the point B. The cool, dry NE advection is seen throughout the lowest 2 km, in the first case. It begins at around 24 hours of the simulation, i.e. at 00 UTC on 4 February, near the ground and up to around 250 m high. After additional 12 hours the cooling continues in the column higher up and it takes 6 hours to reach 2 km high. In the second case there are nearly no changes in the temperature near the surface. There is however strong stabilization of the atmosphere aloft.

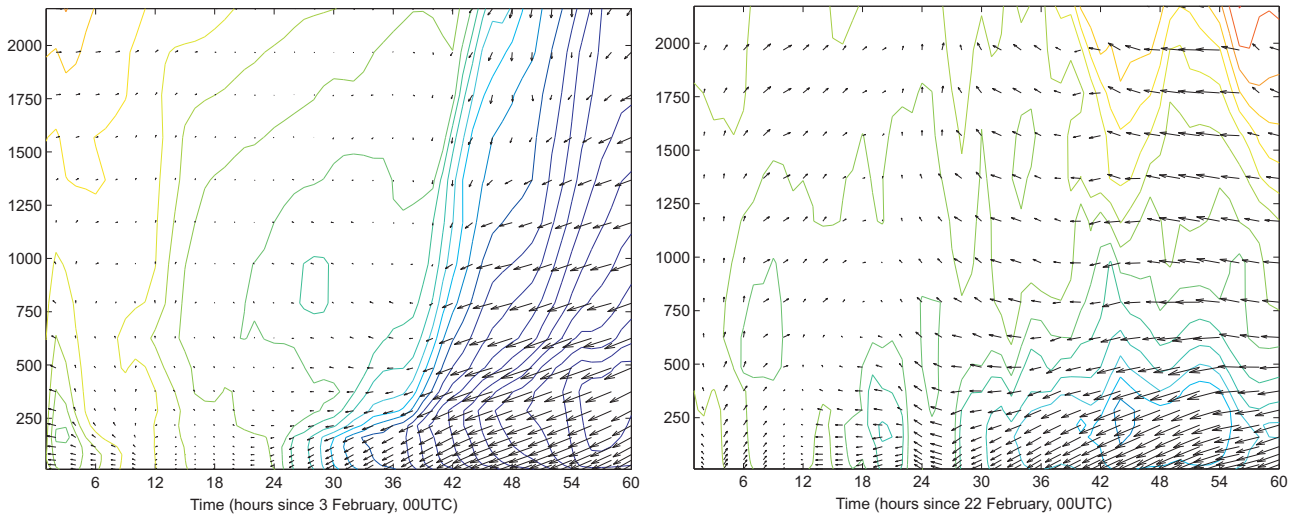

Figure 3: Simulated time evolution of the θ_e profile, relative to the surface value at 24 hours (colored contours in 0.5 K interval), and the vertical profile of the horizontal wind vector (maximum length corresponds to 16 ms^{-1}) for the column of air above location B in Fig. 2.

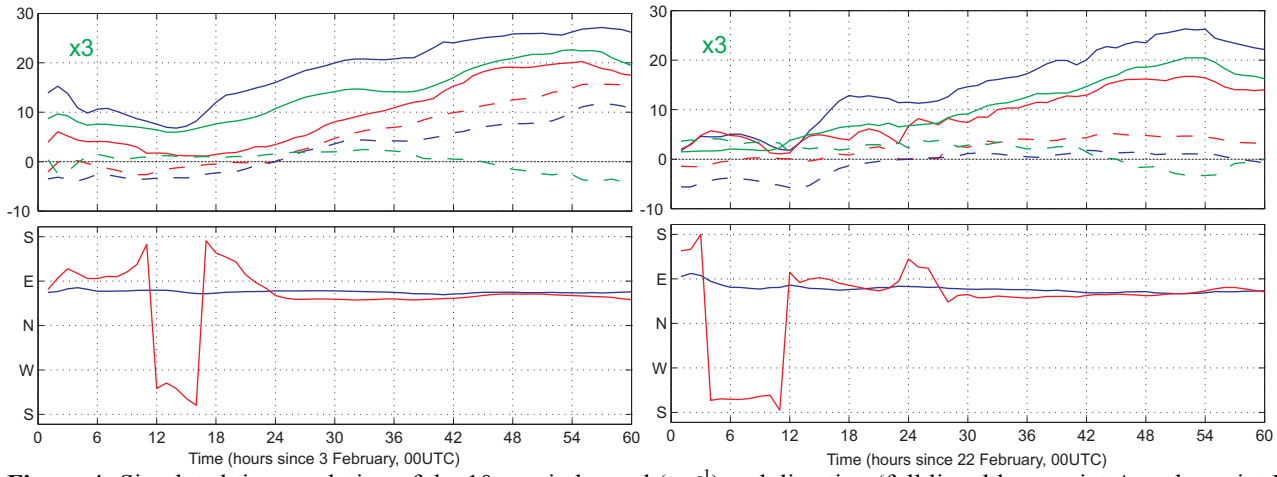

Figure 4: Simulated time evolution of the 10 m wind speed (ms^{-1}) and direction (full line, blue - point A, red – point B; direction in the lower two panels), the θ_e (K) decrease from the value at 24 hours at the lowest model level, i.e. at 10 m above the surface (dashed line, blue – point A, red – point B), and the three-times the mean sea-level pressure difference (hPa) between the points C and A (full green line) and between A and B (dashed green line).

Figure 4 summarizes the differences and similarities between the two cases. Correlation coefficient for the whole simulation, between the wind speed and across-ridge pressure gradient (between points C and A) for the case of 4 February, i.e. with deep NE flow, is 0.9627 for the coastal point (A in Fig. 2) and 0.9684 for the point 80km offshore (B in Fig. 2). For the second case with warm air aloft the correlation coefficient between the wind speed and across-ridge pressure gradient is even higher, 0.9837 for the coastal point and nearly exactly the same, 0.9680 for the offshore point. Comparing to the first case this difference is indicative and pointing to other processes than just the pressure gradient affecting the development offshore. On the other hand the pressure difference between the points A and B, i.e. pressure at the coast minus that offshore, bears no correlation with either wind speed or temperature in any of the two cases. Perhaps noteworthy is the reversal of this difference at around 45 hours in the simulation in both cases, although the surface temperature difference is almost constant around 3 K in favor of the offshore point and there are no significant changes in the wind speed.

Next we compare the evolution of the low level equivalent potential temperature at points at the coast and offshore, and its relation to the wind speed. A significant difference occurred between the two cases. In the first case the increase of the wind speed is accompanied by the decrease in the temperature, at both points, which is

of course consistent with the cold advection, seen in Fig. 3. In the second case, however, the temperature deviates much less, especially at the coast.
Finally we focus to the correlation between the equivalent potential temperature at the surface at points A and B and that at the various heights above point C. If θ_e is considered nearly constant for a trajectory, the height of origin of the later could be defined. It is found that in the first case of a deep NE flow the origin is probably (correlation 0.99) at the height of around 1700 m, which is a few hundred meters above the top of the ridge between points C and A. In the second case the height of best correlation is similar, but the correlation is only as high as 0.6. A detailed analysis of trajectories for the second case shows that during the episode the origin of the air reaching point B is slowly shifting from above the middle Adriatic basin towards the east. The air then makes a left turn at roughly the same altitude until above the ridge between points C and A, and then accelerates downwards and finally continues towards point B. Since the air never crosses the column above point C the weak correlation between C and A can thus be explained. This also explains why the temperature at point B remains almost constant, although the temperature at the continent drops by around 5 K during the episode. In the first case the drop in temperature offshore and at the continent is almost equal, around 9 K.
It should be noted that during the period of strong bora wind the path of air parcels reaching point B fluctuates very little from the straight line AB in either of the two cases studied.

3. CONCLUSIONS

The analysis of the two quite different bora episodes in terms of the background atmospheric state shows that the wind speed offshore, 80 km from the acceleration region correlates strongly to the pressure gradient across the mountain barrier, regardless of whether the pressure at the continent rises more than above the sea or the pressure at the sea falls more than at the continent.
Further it was found from the temperature analysis and from the trajectory analysis that the mid-tropospheric air can join the accelerating streamline first above the ridge, and then continue its journey within the bora flow towards offshore. In such a case bora wind can have equal speeds as in the case of a deep cold airmass rushing into the Adriatic basin from the NE.

REFERENCES

Enger, L. and Grisogono, B. 1998: The response of bora-type flow to the sea surface temperature. *Q. J. R. Meteorol. Soc*., **124**, 1227-1244.
Hodur, R.M., 1997: The Naval Research Laboratory's Coupled Ocean/Atmosphere Mesoscale Prediction System (COAMPS). *Mon. Wea. Rev.* **125**, 1414-1430.